Materials Letters 182 (2016) 47–51

Contents lists available at ScienceDirect

Materials Letters

journal homepage: www.elsevier.com/locate/matlet

Soft-template assisted synthesis of mesoporous CuO/Cu_2O composite hollow microspheres as efficient visible-light photocatalyst

Jiangyao Chen [a,1], Xiaolu Liu [a,c,1], Haimin Zhang [b,d], Porun Liu [b], Guiying Li [a], Taicheng An [a,*], Huijun Zhao [b,*]

[a] State Key Laboratory of Organic Geochemistry and Guangdong Key Laboratory of Environmental Protection and Resources Utilization, Guangzhou Institute of Geochemistry, Chinese Academy of Sciences, Guangzhou 510640, China
[b] Centre for Clean Environment and Energy, Griffith University, Gold Coast Campus, QLD 4222, Australia
[c] University of Chinese Academy of Sciences, Beijing 100049, China
[d] Key Laboratory of Materials Physics, Centre for Environmental and Energy Nanomaterials, Anhui Key Laboratory of Nanomaterials and Nanotechnology, Institute of Solid State Physics, Chinese Academy of Sciences, Hefei 230031, China

ARTICLE INFO

Article history:
Received 11 September 2015
Received in revised form
30 May 2016
Accepted 19 June 2016
Available online 20 June 2016

Keywords:
Porous materials
Semiconductors
Soft-template assisted method
Solar energy materials
Dye pollutant

ABSTRACT

Highly efficient visible-light-active CuO/Cu_2O heterostructured composite hollow microspheres were successfully developed under an appropriate molar ratio of the copper precusor to the reductant – D-sorbitol for photocatalytic degradation of methyl orange with outstanding photostability. The hollow microsphere structure composite displayed high visible-light photocatalytic activity and reproducibility toward the degradation of methyl orange, due to its high adsorption capacity, enhanced light scattering effects, high throughput hollow reaction regions within the hollow structures and decreased recombination of photogenerated electrons and holes. This demonstrated useful hollow microspheres act as an example of developing highly efficient heterostructured binary metal oxides for photocatalytic water purification.

1. Introduction

CuO and Cu_2O semiconductors with narrow bandgaps have received much attention in recent years because of their various promising applications in environmental remediation and energy production [1,2]. In consideration of their potential applications, CuO or Cu_2O materials with various hollow structures have been also attempted [3,4], which show higher surface area and porosity, greater light-harvesting capacity and higher photocatalytic activity for pollutant degradation than their particulate counterparts [5]. Moreover, in contrast to single one, the bi-component metal oxides integrating two types of functional materials show higher photocatalytic efficiency owing to increased charge separation capability and extended energy range of photoexcitation [6,7]. In fact, CuO/Cu_2O composite hollow structures photocatalyst offers enhanced activities over their single counterparts [8,9]. However, no reports on synthesis of CuO/Cu_2O composite hollow structures for the application in the environmental remediation under visible light irradiation have been attempted yet [10].

Besides, the stability of a given photocatalyst is a crucial factor for its practical application. Cu_2O has been reported possessing poor stability in aqueous solution under light illumination [11,12], while CuO is a very stable phase of copper oxide and can be successfully used as a protection layer to keep Cu_2O from photocorrosion [13]. Unfortunately, the investigation of photostability of CuO/Cu_2O composite hollow structures has not been concerned yet. Therefore, the fabrication of CuO/Cu_2O composite hollow structures with highly visible-light-driven photocatalytic activity and good stability is highly desirable. Meanwhile, to fabricate the hollow structure photocatalysts, the template-directed approaches have been demonstrated to be effective methods, while the soft template method is more advantageous than hard template one owing to negligible external template and post-treatment process [14,15].

In this work, the synthesis of CuO/Cu_2O composite hollow microspheres was reported by using a facile soft-template assisted hydrothermal method. The reuslting sample was used as a visible-light-driven photocatalyst for the degradation of organic pollutant, exhibiting high photocatalytic efficiency and good stability.

* Corresponding authors.
E-mail addresses: antc99@gdut.edu.cn (T. An), h.zhao@griffith.edu.au (H. Zhao).
[1] Both authors contributed equally to this work and were considered as co-first authors.

http://dx.doi.org/10.1016/j.matlet.2016.06.077
0167-577X/

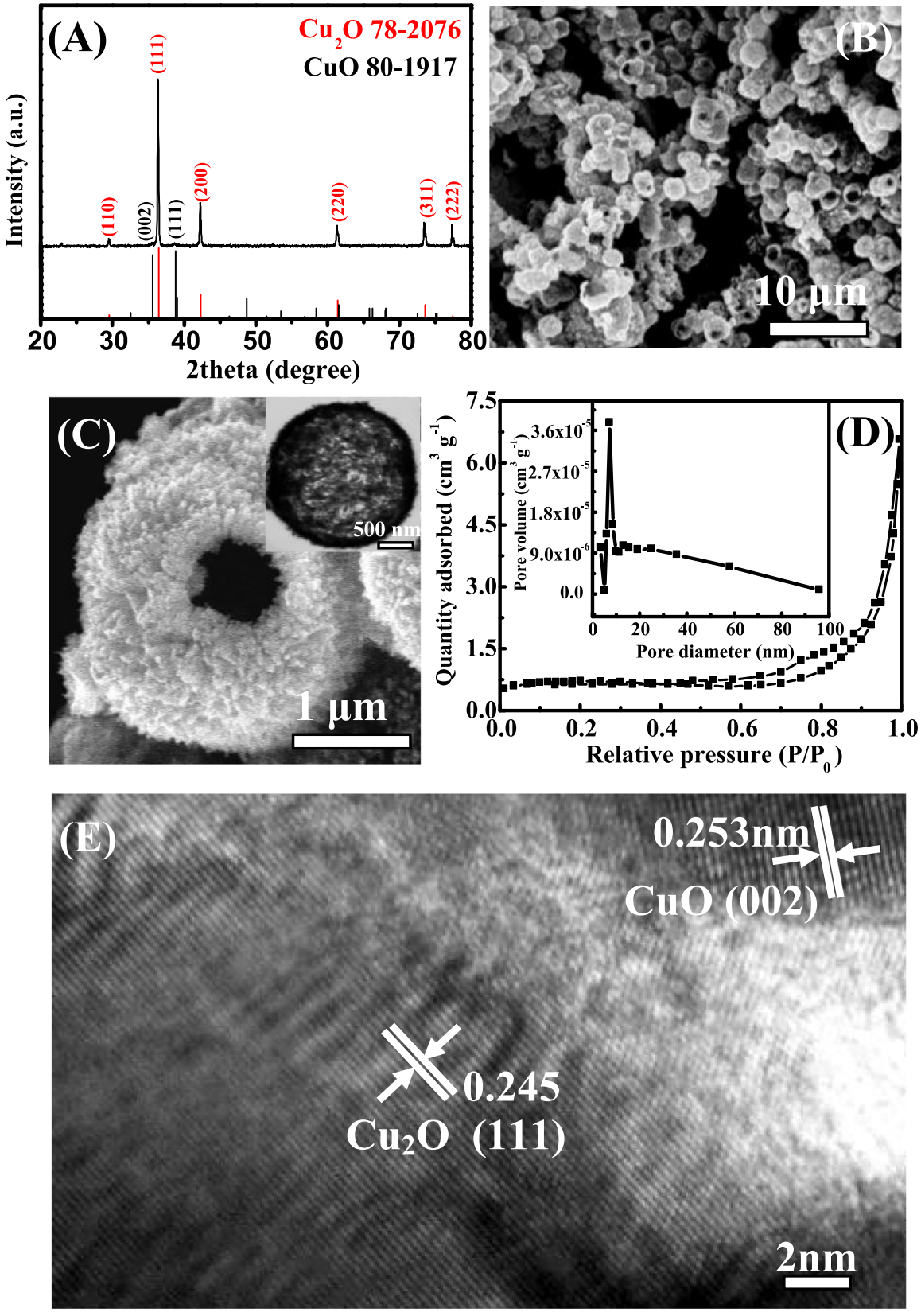

Fig. 1. XRD (A), SEM (B), TEM (C), N_2 adsorption-desorption isotherm and pore size distribution curve (D) and high resolution TEM (E) data of the prepared CuO/Cu_2O composite hollow microspheres.

2. Experimental

2.1. Synthesis procedure

In a typical synthesis procedure, appropriate amounts of $Cu(CH_3COO)_2 \cdot H_2O$ and D-sorbitol were added into a 5 g L^{-1} Pluronic P123 aqueous solution under vigorous stirring, and the molar ratio of $Cu(CH_3COO)_2 \cdot H_2O$ to D-sorbitol was 10:1. The mixed solution was then transferred into a 60 mL Teflon container for hydrothermal treatment under 150 °C for 24 h. After that, the precipitation was collected and then washed with distilled water for three times. Microwave-assisted extraction was used to remove the template from the as-prepared samples dispersed in ethanol and finally air-dried overnight at 55 °C.

2.2. Characterization

The crystallographic information of the prepared samples was established by X-ray diffraction (XRD, Rigaku D/MAX-2200 VPC). The morphology and microstructure were characterized using a field emission scanning electron microscopy (SEM, JOEL JSM-890) and a transmission electron microscopy (TEM, Philips F20). Nitrogen adsorption-desorption isotherm was obtained with a Micromeritics ASAP 2020 system. Surface data was obtained using X-ray photoelectron spectroscopy (XPS, Thermo ESCALAB 250). UV–visible (UV–vis) diffuse reflectance spectra were recorded on a UV–vis–NIR spectrophotometer (HITACHI U-3010). The isothermal adsorption and photocatalytic activity for the visible light degradation of methyl orange (MO) was evaluated and the characterization details were provided in the Supporting information.

3. Results and discussion

XRD pattern of a typical sample shown in Fig. 1A reveals that all the diffraction peaks can be assigned to Cu_2O and CuO with the content ratio for Cu_2O to CuO of *ca.* 23:1, indicating the dominant Cu_2O phase. Meanwhile, the sample consists of high-purity hollow microspheres with an average diameter of *ca.* 2.0 μm and a shell thickness of *ca.* 200 nm (Fig. 1B-C). Interestingly, the shell of hollow microsphere is porous and composed of numerous nano-sized crystallines. The N_2 adsorption-desorption isotherm confirms a type IV (IUPAC classification) isotherm with a typical H3 hysteresis loop [16], indicating the existence of mesoporous structure and slit-like pores (Fig. 1D). The pore size ranges from 4.0 to 100 nm, confirming the presence of many mesopores (inset of Fig. 1D). High resolution TEM image reveals the interlayer distance of 0.245 nm and 0.253 nm, agreeing well with the (111) and (002) lattice planes of Cu_2O and CuO, respectively (Fig. 1E). All these results indicate that the mesoporous CuO/Cu_2O composite hollow microspheres are successfully synthesized by using a facile soft-template assisted hydrothermal method.

The template plays a significant role in the formation of well-defined hollow microspheres. In the absence of P123, only CuO/Cu_2O composite aggregates are obtained (Fig. S1). Copper precursor is also found to be crucial that CuO/Cu_2O composite hollow microspheres is obtained when $Cu(CH_3COO)_2 \cdot H_2O$ is used, and bulky particles are obtained in the resultant sample composed of CuO and $Cu(OH)_2$ (or mixed Cu_2O and $Cu_3SO_4(OH)_4$) when $Cu(NO_3)_2 \cdot 3H_2O$ (or $CuSO_4$) is used as the copper precursor (Fig. 2A and S2A-S2B).

In addition, the molar ratio of $Cu(CH_3COO)_2 \cdot H_2O$ to D-sorbitol

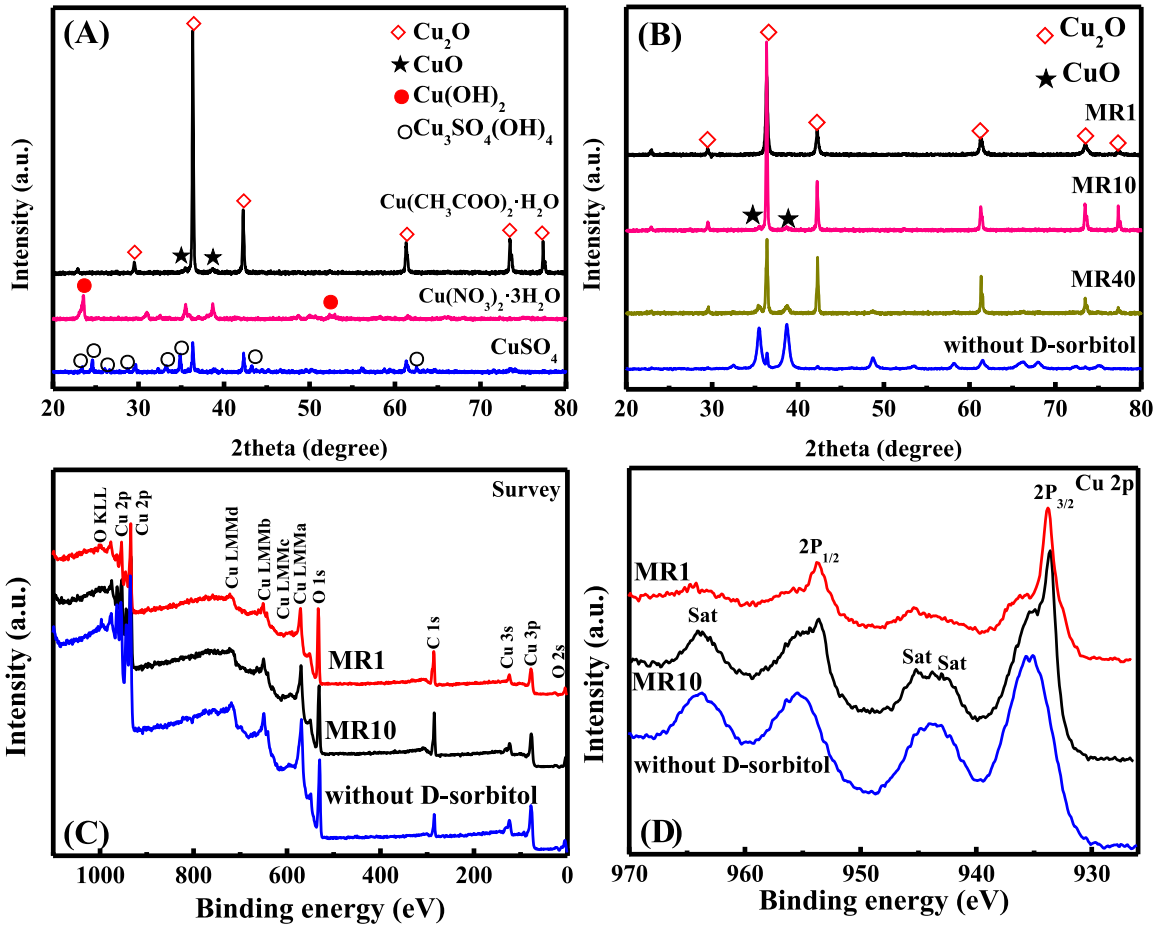

Fig. 2. XRD (A-B) and XPS (C-D) patterns of the samples prepared from different copper precursors and MR.

(assigned as MR) is found as another significant synthesis parameter. When the D-sorbitol is absent (Fig. 2B), characteristic peaks for CuO (002) and (111) planes ($2\theta=35.6°$ and 38.7°) as well as Cu_2O (111) plane ($2\theta=36.4°$) are observed. The content ratio of Cu_2O to CuO equals to 0.4:1, indicating that the sample is the CuO/Cu_2O composite with dominant CuO phase. However, when a little amount of D-sorbitol is added (MR40), a sharp increase of the content ratio of Cu_2O to CuO (*ca.* 7:1) is observed, which further increases to *ca.* 23:1 when the amount of D-sorbitol continuously increases (MR10, Fig. 1A). And only Cu_2O is obtained when the MR decreases to 1:1. In the case of Cu 2p XPS spectrum of the sample prepared without D-sorbitol and with suitable MR (taking MR10 as an example) (Fig. 2C-D), peaks at 933.5 and 953.5 eV suggest the existence of Cu_2O, while those at 935.3 and 955.4 eV are consistent to the peaks of CuO [17,18]. Moreover, the spectra of these samples display several strong satellite peaks between Cu $2p_{3/2}$ peak and

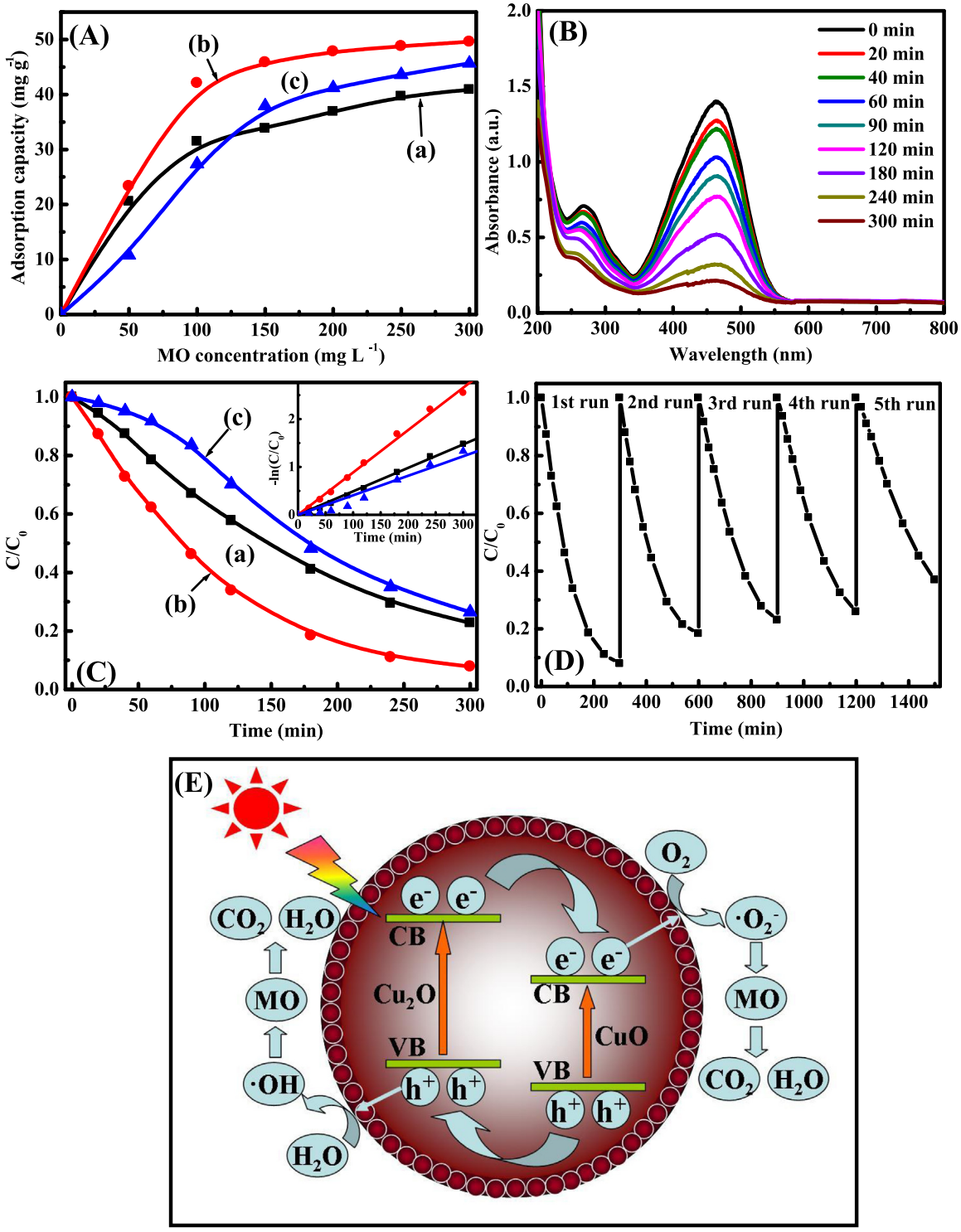

Fig. 3. Adsorption isotherms (A) and photocatalytic degradation (C) of MO on the prepared samples ((a) Cu_2O particles, (b) CuO/Cu_2O composite hollow microspheres and (c) CuO/Cu_2O composite solid microspheres). Absorption spectra of MO at different time (B), stability test (D) and schematic diagram of the enhanced photocatalytic mechanism (E) on CuO/Cu_2O composite hollow microspheres.

its first satellite on the higher enery side of about 8 eV, which is the characteristic of the material such as CuO having a d^9 configuration in ground state [19,20], further proving the existence of CuO. However, two peaks at 933.5 and 953.5 eV without satellite peaks are observed for the sample prepared with MR1, indicating the only existence of Cu_2O. Notably, the peaks for Cu_2O become stronger with the decrease of the intensity of the peaks for CuO as the MR increases, confirming the increase of the content ratio of Cu_2O to CuO. Obviously, only appropriate molar ratio of copper precusor to the reductant-D-sorbitol leads to the formation of mixed CuO and Cu_2O composite. Moreover, sample prepared with the MR1 (without D-sorbitol or MR40) shows solid bulky particles (solid microspheres) (Fig. S2C-S2D), further confirming that the well-defined CuO/Cu_2O composite hollow microspheres can only be obtained when the MR is 10.

Fig. 3A shows the adsorption isotherms of MO on the prepared samples. For Cu_2O particles, the adsorption capacity of MO is 40.9 mg g^{-1}, which increases to 45.7 and 49.6 mg g^{-1} for CuO/Cu_2O composite solid microspheres and hollow microspheres, indicating that CuO/Cu_2O composite hollow microspheres show the highest adsorption capacility toward MO. The lamp is then swiched on to evaluate their photocatalytic activies under visible light irradiation (Fig. S3). As shown in Fig. 3B, the real-time UV–vis spectrum depicts that the absorption peaks corresponding to MO (463 nm) disappear obviously within 300 min illumination, indicating that the MO is effectively degraded by the prepared CuO/Cu_2O composite hollow microspheres under visible light irradiation. One of the possible reasons may be due to the enhanced visible light scattering of the prepared CuO/Cu_2O composite hollow microspheres (Fig. S4). Moreover, after 300 min irradiation, approximate 77.3%, 73.6% and 92.2% of MO is degraded by Cu_2O particles, CuO/Cu_2O composite solid microspheres and CuO/Cu_2O composite hollow microspheres, respectively (Fig. 3C), and the best degradation effciency can be obtained for CuO/Cu_2O composite hollow microspheres. Moreover, the degradation rate for the CuO/Cu_2O composite hollow microspheres (0.0089 min^{-1}) is almost 1.8 and 2.2 times to Cu_2O particles (0.0049 min^{-1}) and CuO/Cu_2O composite solid microspheres (0.0041 min^{-1}), further confirming the highest photocatalytic activity of CuO/Cu_2O composite hollow microspheres (inset of Fig. 3C). Meanwhile, photostability test is conducted and the result demonstrates that after five repeated use, 63.1% of the degradation efficiency can still be obtained, indicating the relatively good photostability of the fabricated CuO/Cu_2O composite hollow microspheres photocatalyst (Fig. 3D). The decrease of the degradation efficiency may be contributed to the generation of refractory intermediates on the catalyst.

The superiorly visible-light-driven photocatalytic activity and stability for the prepared photocatalyst can be attributed to its high adsorption capacity, enhanced light scattering effects, high throughput hollow reaction regions within the hollow structures and decreased recombination of photogenerated electrons and holes (Fig. 3E). Firstly, due to its high visible light absorption capability and porous shell structure, both visible light and MO moleculars are more conveniently penetrated into it with the significantly accelerated diffusion velocity and reaction rate. For instance, the molecular size of MO is 1.19 nm × 0.67 nm × 0.38 nm [21], leading to the easy entrance and diffusion of MO molecules into the pores of catalyst (pore size: 4.0–100 nm). Secondly, its unique micro-sized hollow structure can also provide high throughput hollow reaction regions, not only enhancing the light harvesting and scattering, but also facilitating the transfer and diffusion of dye molecules [5]. Thirdly, the existense of CuO can serve as a protector minimizing Cu_2O photocorrosion [13]. Meanwhile, the interface between the Cu_2O and CuO acts as a rapid separation site for the photogenerated electrons and holes, due to the difference in the energy levels of their conduction bands and valence bands [8,9], leading to the high utilization of the absorbed visible light.

4. Conclusions

In summary, CuO/Cu_2O composite hollow microspheres photocatalyst with highly visible light photocatalytic activity and photostability toward degradation of dye pollutant is fabricated. The improved photocatalytic performance is attributed to its high adsorption capacity, enhanced light scattering effects, high throughput hollow reaction regions within the hollow structures, and decreased recombination of photogenerated electrons and holes. This study will deepen the understanding of the enhanced photocatalytic mechanism of bi-component metal oxides photocatalysts and promote their practical application in environmental remediation.

Acknowledgements

The authors appreciate the financial supports from NSFC (41373102, 21307132 and U1401245), Pearl River S&T Nova Program of Guangzhou (201506010077), National Natural Science Funds for Distinguished Young Scholars (41425015) and Guangdong Natural Science Foundation (S2013040016408).

Appendix A. Supplementary material

Supplementary data associated with this article can be found in the online version at http://dx.doi.org/10.1016/j.matlet.2016.06.077.

References

[1] M. Sabbaghan, J. Beheshtian, R.N. Liarjdame, Mater. Lett. 153 (2015) 1–4.
[2] X.Q. Ge, H.M. Hu, C.H. Deng, Q. Zheng, M. Wang, G.Y. Chen, Mater. Lett. 141 (2015) 214–216.
[3] Y.M. Sui, W.Y. Fu, Y. Zeng, H.B. Yang, Y.Y. Zhang, H. Chen, et al., Angew. Chem. Int. Ed. 49 (2010) 4282–4285.
[4] C.H. Kuo, M.H. Huang, J. Am. Chem. Soc. 130 (2008) 12815–12820.
[5] J.Y. Chen, X. Nie, H.X. Shi, G.Y. Li, T.C. An, Chem. Eng. J. 228 (2013) 834–842.
[6] A. Enesca, L. Isac, A. Duta, Thin Solid Films 542 (2013) 31–37.
[7] M.L. Zhang, T.C. An, X.H. Hu, C. Wang, G.Y. Sheng, J.M. Fu, Appl. Catal. A-Gen. 260 (2004) 215–222.
[8] S.L. Wang, P.G. Li, H.W. Zhu, W.H. Tang, Powder Technol. 230 (2012) 48–53.
[9] H.G. Yu, J.G. Yu, S.W. Liu, S. Mann, Chem. Mater. 19 (2007) 4327–4334.
[10] A. Sharma, M. Varshney, J. Park, T.K. Ha, K.H. Chae, H.J. Shin, RSC Adv. 5 (2015) 21762–21771.
[11] H.W. Wu, S.Y. Lee, W.C. Lu, K.S. Chang, Appl. Surf. Sci. 344 (2015) 236–241.
[12] A. Paracchino, V. Laporte, K. Sivula, M. Gratzel, E. Thimsen, Nat. Mater. 10 (2011) 456–461.
[13] Z.H. Zhang, P. Wang, J. Mater. Chem. 22 (2012) 2456–2464.
[14] Z.X. Wei, L.J. Zhang, M. Yu, Y.S. Yang, M.X. Wan, Adv. Mater. 15 (2003) 1382–1385.
[15] L. Ren, K. Li, X.F. Chen, Polym. Bull. 63 (2009) 15–21.
[16] T.C. An, J.Y. Chen, X. Nie, G.Y. Li, H.,M. Zhang, X.L. Liu, et al., ACS Appl. Mater. Inter 4 (2012) 5988–5996.
[17] Y.J. Xiong, Z.Q. Li, R. Zhang, Y. Xie, J. Yang, C.Z. Wu, J. Phys. Chem. B 107 (2003) 3697–3702.
[18] J. Morales, J.P. Espinos, A. Caballero, A.R. Gonzalez-Elipe, J.A. Mejias, J. Phys. Chem. B 109 (2005) 7758–7765.
[19] W.T. Yao, S.H. Yu, Y. Zhou, J. Jiang, Q.S. Wu, L. Zhang, et al., J. Phys. Chem. B 109 (2005) 14011–14016.
[20] Y.C. Zhang, J.Y. Tang, G.L. Wang, M. Zhang, X.Y. Hu, J. Cryst. Growth 294 (2006) 278–282.
[21] J.H. Huang, K.L. Huang, S.Q. Liu, A.T. Wang, C. Yan, Colloid Surf. A 330 (2008) 55–61.